Combined ESR and Thermodynamic Studies of the Superoxide Adduct of 5-(Diethoxyphosphoryl)-5-Methyl-1-Pyrroline *N*-Oxide (DEPMPO): Hindered Rotation around the O−O Bond Evidenced by Two-Dimensional Simulation of Temperature-Dependent Spectra

Antal Rockenbauer,[†] Jean-Louis Clément,[‡] Marcel Culcasi,*[,‡] Anne Mercier,[‡] Paul Tordo,[‡] and Sylvia Pietri[‡]

Chemical Research Center, Institute of Structural Chemistry, H-1025 Budapest, Pusztaszeri út 59, Hungary, and Laboratoire Structure et Réactivité des Espèces Paramagnétiques−Sondes Moléculaires en Biologie, CNRS-UMR 6517, Universités d'Aix-Marseille 1 et 3, Faculté des Sciences de Saint-Jérôme (case 522), 13397 Marseille Cedex 20, France

Received: January 26, 2007; In Final Form: April 4, 2007

Experiments were performed to elucidate the origin of the superhyperfine structure and line width alternation (LWA) seen in the ESR spectrum of the major diastereoisomer (**1**) of DEPMPO-OOH, the remarkably persistent superoxide adduct of 5-(diethoxyphosphoryl)-5-methyl-1-pyrroline *N*-oxide (DEPMPO). Using selectively deuterated DEPMPO derivatives, we demonstrated that the superhyperfine pattern can be unambiguously attributed to long-range couplings. The recording in pyridine of highly resolved spectra in a wide temperature range, combined with two-dimensional simulation, allowed us to characterize an inverted LWA in **1** and revealed a uniform line broadening in the spectrum of the minor DEPMPO-OOH diastereoisomer (**2**), with both effects originating from a chemical exchange between conformers. When the individual spectra of **1** presenting LWA in the fast-exchange regime were simulated, four equally good fits were obtained and this ambiguity could be resolved by using a two-dimensional simulation technique. The thermodynamic and kinetic constants of this exchange were consistent with a rotation around the O−O bond. We propose that line broadening effects in **1** and **2** result from this O−O rotation concerted with the pseudo-rotation of the pyrrolidine ring.

1. Introduction

The variation of line width in the hyperfine pattern of ESR spectra bears crucial information about molecular dynamics. This phenomenon has been extensively studied in the case of nitroxides probes or spin labels, having outstanding applications in the evaluation of motional parameters of biological systems.[1] The origin of line broadening occurs along with certain dynamic phenomena such as molecular reorientational tumbling partially averaging the anisotropy of the *g* and *A* tensors, or the intramolecular conversion between conformations. This latter situation, termed as chemical exchange, results in line width alternation (LWA) in the hyperfine pattern, provided at least two nuclei have rather different hyperfine coupling constants (hfcs) in the interconverting species. Such unusual shape of the ESR spectra is generally an unwanted feature in spin trapping, where nitroxide spin adducts are intended to unequivocally provide structural and quantitative information on the primary radical species formed. Very typical of this situation are the hydroperoxyl radical adducts of five-membered ring nitrones such as 5,5-dimethyl-1-pyrroline *N*-oxide (DMPO, Scheme 1A), in particular, 2,2-dimethyl-5-hydroperoxy-1-pyrrolidinyloxyl (DMPO-OOH, Scheme 1A), the protonated DMPO adduct of superoxide ($O_2^{\bullet-}$). The X-band ESR signal of DMPO-OOH was first reported more than 30 years ago,[2] being composed of 12 lines with hfcs consistent with nitrogen, β-hydrogen, and one long-range hydrogen. However, the DMPO-OOH spectrum cannot be simulated as a unique species because of its asymmetry, the origin of which has been a matter of debate.[3−7] The main difficulty in correctly modeling the ESR line shapes of DMPO-OOH results from its intramolecular decay pattern forming the more persistent 2,2-dimethyl-5-hydroxy-1-pyrrolidinyloxyl (DMPO-OH), the DMPO adduct of hydroxyl radical ($HO^{\bullet}$), whose quartet spectrum superimposes to that of DMPO-OOH within seconds at room temperature.[8] Despite a technique to produce DMPO-OOH virtually devoid of any contamination with DMPO-OH having been reported,[9] the resulting DMPO-OOH signals nevertheless retain asymmetry, which therefore appears to be intrinsic to the nitroxide. At room temperature, this line asymmetry may be imitated considering either the existence of two superimposed signals from different species[3,4] or a slow intramolecular chemical exchange,[5,10] but only in the latter case was a hfcs of about 0.12 mT from one hydrogen atom of C-3 introduced in the calculation. Using DMPO derivatives either fully deuterated or ^{2}H-substituted at C-2 and C-3 (DMPO-d_3, Scheme 1A), Pou et al.[11] first obtained direct evidence for the contribution of one C-3 γ-hydrogen coupling to the spectrum pattern of DMPO-OOH. This was definitively confirmed in our laboratory, because DMPO selectively deuterated at C-3 (DMPO-d_2, Scheme 1A) yields a symmetrical ESR sextet upon trapping of $O_2^{\bullet-}$ and we therefore assumed that it is the significant difference (calculated as 0.14 mT) in γ-couplings between two exchanging conformers of DMPO-

* Corresponding author. Tel: (33) 4 91 28 90 25. Fax: (33) 4 91 28 87 58. E-mail: culcasi@srepir1.univ-mrs.fr.
[†] Institute of Structural Chemistry.
[‡] Universités d'Aix-Marseille 1 et 3.

10.1021/jp070679u CCC: $37.00
Published on Web 05/23/2007

SCHEME 1: Structures of Nitrones and Related Spin Adducts

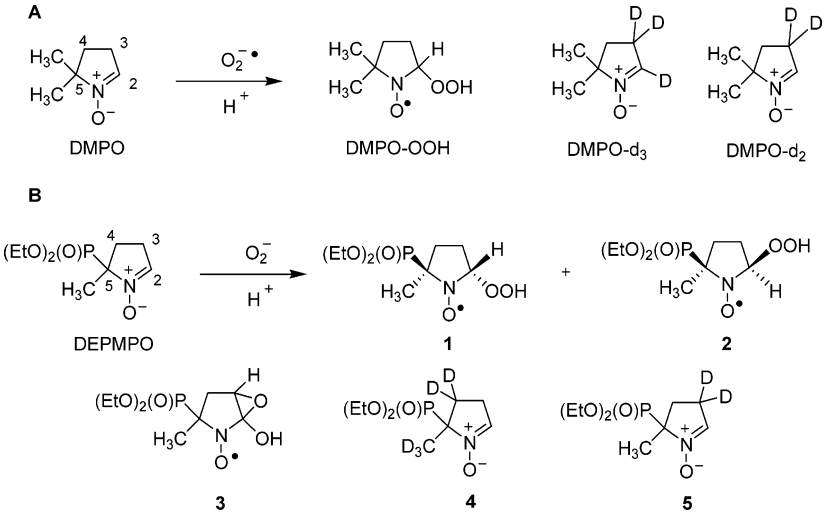

OOH that causes spectral asymmetry[5] with no LWA. As additional support for the hypothesis of interconverting conformers, a temperature-dependence of the DMPO-OOH spectral asymmetry was recently reported.[6]

In our search for spin traps yielding $O_2^{\bullet-}$ adducts more persistent than DMPO-OOH, we,[10,12] followed by others,[13] have developed a new family of pyrroline *N*-oxides bearing at least one ^{31}P-containing substituent at C-5, the most popular compound in biological studies still being 5-(diethoxyphosphoryl)-5-methyl-1-pyrroline *N*-oxide (DEPMPO, Scheme 1B). Many of the DEPMPO-type nitrones (DEPMPOs) reported to date meet the stability criterion stated above, the half-life of the $O_2^{\bullet-}$ adducts being 8−20 times larger than that of DMPO-OOH.[10,12,13] Meanwhile, two main difficulties are encountered in the spectral simulation of DEPMPOs-OOR adducts (R = H or alkyl).

First, regardless of their mechanism of formation, they are often obtained as mixtures of cis/trans diastereoisomers as a consequence of nonstereoselective radical addition on both diastereotopic faces of the parent nitrones. Scheme 1B depicts the situation for 2-diethoxyphosphoryl-2-methyl-5-hydroperoxy-1-pyrrolidinyloxyl (DEPMPO-OOH), the $O_2^{\bullet-}$ adduct of DEPMPO. We assigned the major diastereoisomer to *trans*-DEPMPO-OOH (**1**), because the enantiomeric excess found in DEPMPOs-OOR (R = H or alkyl) seems to depend upon steric hindrance around the nitrone function,[10,12,13] e.g., using a standard $O_2^{\bullet-}$ generator at room temperature, *cis*-DEPMPO-OOH (**2**) typically accounts for only 7% in the mixture.[14] According to computations by Villamena et al., however, a hydrogen bond specific to **2** can invert the formation probabilities, making this diastereoisomer the preferential adduct.[15]

Second, in addition to spectral asymmetry similar to that of DMPO-OOH, the major *trans*-DEPMPOs-OOR signals exhibit a spectacular LWA and, if adequate acquisition settings are used, superhyperfine resolution of the sharpest lines.[6,10,12c−g,13a]

Because it could not be explained by any proton exchange mechanism[10] and it was not observed in DEPMPOs-OR adducts[12d,13a,b,16], an explanation[10] for LWA in the major *trans*-DEPMPOs-OOH and DEPMPOs-OOR ESR signals involved intramolecular conformational changes within the pyrrolidine ring associated with restricted rotation of the peroxyl bond.[17] In the case of **1** in aqueous medium, the best simulations of highly resolved spectra were consistent with two individual conformers having significant differences in their β-H and ^{31}P hfcs of 0.36 mT and 0.63 mT, respectively, thus being at the origin of LWA.[14] In this study[14] the observed superhyperfine structure of DEPMPO-OOH was best simulated assuming two conformers for **1** having γ-couplings in the range 0.09−0.05 mT. An alternative model was recently proposed in which this superhyperfine structure was attributed to the β-epoxy ring-containing nitroxide **3**, considered as a decomposition product of **1** (Scheme 1B).[6]

In this paper, we used selective deuterium labeling of DEPMPO and $O_2^{\bullet-}$ spin trapping as a model of DEPMPOs-OOR adducts to assess the participation in the ESR signal of a nitroxide bearing only one γ-hydrogen at C-3, such as in **3**. We then carried out experimental conditions allowing to record high-resolution spectra of mixtures of **1** and **2** in a wide temperature range, and a two-dimensional simulation procedure[18] to investigate the existence of chemical exchange for both diastereoisomers and extract their thermodynamic parameters.

2. Experimental Section

Pyridine from Acros Organics was freshly distilled and stored over potassium hydroxide. Other solvents, starting materials, and reagents were of laboratory reagent grade from Acros Organics or Sigma-Aldrich. Water was produced with an Elga Purelab Option deionizer. DEPMPO and its pentadeutero (**4**) or selectively C-3 deuterated (**5**) analogues (Scheme 1) were prepared and purified by published procedures.[10,19] Isotopic purity was estimated >95% by ^{1}H NMR. ESR measurements were carried out in either a cylindrical tube or a standard aqueous flat cell using a Bruker ESP 300 X-band spectrometer equipped with a ER 4111 VT, calibrated (±2 °C) variable temperature unit, a ER 053M gaussmeter, a Hewlett-Packard 5350B frequency counter, a TM110 cavity, and a 100-kHz field modulation. Samples set at a given temperature are allowed to stabilize for at least 2 min prior to ESR acquisition. Sample solutions in aqueous KH_2PO_4 buffer (0.16 M; pH 7.0) contained 0.9 mM diethylenetriaminepentaacetic acid (DTPA), 10% v/v dimethyl sulfoxide (DMSO), 0.01 M 18-crown-6 ether (1,4,7,-10,13,16-hexaoxacyclooctadecane), 0.05 M nitrone, and 0.01 M potassium superoxide (KO_2) as the $O_2^{\bullet-}$ generator and were bubbled with nitrogen gas for 45 s prior to spectral acquisition. Sample solutions in anhydrous pyridine contained DEPMPO (0.1 M) and 0.32 M of hydrogen peroxide (H_2O_2) from a 30% aqueous solution and were bubbled with air for 3 min and then deoxygenated by freeze/thaw cycles before heating. ESR spectra were sequentially simulated using a previously described program.[17]

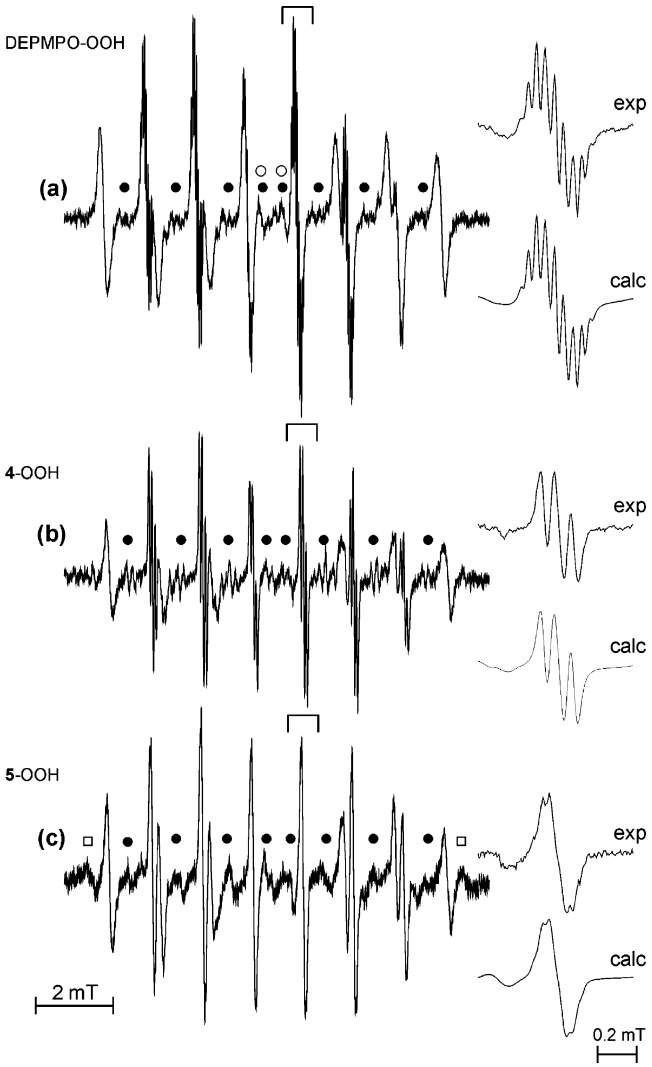

Figure 1. ESR spectra of $O_2^{\bullet-}$ adducts of DEPMPO and its deutero analogues **4** and **5** at 295 K in phosphate buffer. (Left) Experimental spectra showing contributions from the minor cis (●), $HO^{\bullet}$ (○), and alkyl (□) adducts. (Right) Experimental and calculated spectra of the selected region.

3. Results and Discussion

(a) Definitive Assignment of the Superhyperfine Structure of DEPMPO-OOH Using Selective Deuteration. A phosphate buffer reaction of DEPMPO with KO_2 at room temperature produced DEPMPO-OOH that, under low modulation amplitude conditions (i.e., 0.01 mT), yielded the well-known highly resolved ESR spectrum shown in Figure 1a. In this spectrum, the two inner lines in the superhyperfine structure pattern of the major nitroxide clearly consisted of nine lines with a maximal hfcs <0.1 mT, which indicates long-range couplings. However, because of the presence of seven γ-hydrogen atoms in DEPMPO-OOH (Scheme 1), the extent of their contribution to these nine lines is not straightforward. When **4** (5-diethoxyphosphoryl-5-([$^2H_3$]methyl)-[3,3-$^2H_2$]-1-pyrroline *N*-oxide) was used instead of DEPMPO, the superhyperfine structure of the corresponding **4**-OOH adduct was reduced to a triplet (Figure 1b) showing that both γ-hydrogen atoms at C-3 are nonequivalently coupling. This dramatic decrease in the number of parameters to compute facilitated the simulation of the spectrum of Figure 1b and the best fit was obtained assuming (i) the superimposition of the cis and trans diastereoisomers of **4**-OOH (proportions 1:13) with little contamination with 8% **4**-OH (the $HO^{\bullet}$ spin adduct of **4**), and (ii) the existence of a two-site chemical exchange for the major component of **4**-OOH (likely *trans*-**4**-OOH), which produces the LWA seen in the spectrum. The simulated ESR parameters of the spectrum of Figure 1b and the relaxation parameters (see eq 1) for the two T1 and T2 sites of *trans*-**4**-OOH are reported in Table 1, showing that the magnitude of one γ-coupling at C-3 should be at the higher limit of what is expected from the superhyperfine pattern seen in DEPMPO-OOH, i.e., 0.09 mT. In strong support, when $O_2^{\bullet-}$ was spin-trapped by **5** (5-diethoxyphosphoryl-5-methyl-[3,3-$^2H_2$]-1-pyrroline *N*-oxide) LWA was still seen in the ESR spectrum of the main component of **5**-OOH (presumably *trans*-**5**-OOH), but in this case, the superhyperfine structure of the sharpest lines was barely visible (Figure 1c) as a consequence of significant line broadening brought by deuterium substitution at C-3. Considering the structural information extracted from the superhyperfine patterns in **4**-OOH and **5**-OOH spectra, which is that the two hydrogen atoms of C-3 are necessarily coupling, a realistic simulation of LWA in **1** could be performed assuming it arises from a unique radical species subjected to an intramolecular chemical exchange between T1 and T2 sites (Table 1), a hypothesis we put forward earlier.[10,14] In the spectrum of **4**-OOtBu, we have observed[19] a triplet pattern similar to that of Figure 2b. Contrary to a recent proposal,[6] we therefore demonstrate that **3**-type nitroxide bearing only one C-3 hydrogen atom does not participate in the ESR signal of DEPMPO-OOH, and likely in other DEPMPOs-OOR peroxyl adducts. However some decay of these adducts into secondary aminoxyls may

TABLE 1: Simulated ESR Parameters (upper part) and Relaxation Parameters and Exchange Times (lower part) for Superoxide Spin Adducts in Phosphate Buffer at 295 K

						$a_{H\gamma}$[a] (mT)		
nitroxide[b]	species %	conformer	a_N (mT)	a_P (mT)	$a_{H\beta}$ (mT)	3-C	4-C	5-C
1	92	T1 (61.6%)	1.298	5.306	1.262	0.090 (1H)/0.060 (1H)	0.044 (2H)	0.037 (3H)
		T2 (38.4%)	1.310	4.503	0.828	0.090 (1H)/0.060 (1H)	0.044 (2H)	0.037 (3H)
2	8		1.337	4.014	0.988	0.146 (1H)[c]		
trans-**4**-OOH	91	T1 (61.8%)	1.290	5.314	1.262	0.090 (1H)/0.061 (1H)	0.0073 (2D)	0.0063 (3D)
		T2 (38.2%)	1.329	4.506	0.828	0.090 (1H)/0.061 (1H)	0.0073 (2D)	0.0063 (3D)
cis-**4**-OOH	9		1.332	4.023	0.981	0.143 (1H)[c]		
trans-**5**-OOH	90	T1 (61.7%)	1.287	5.339	1.261	0.014 (1D)/0.010 (1D)	0.046 (2H)	0.035 (3H)
		T2 (38.3%)	1.316	4.459	0.846	0.014 (1D)/0.010 (1D)	0.046 (2H)	0.035 (3H)
cis-**5**-OOH	10		1.333	4.080	1.014	0.024 (1D)[c]		

nitroxide	$\tau1$[d] (ns)	$\tau2$ (ns)	α (μT)	β (μT)	γ (μT)	β' (μT)	γ' (μT)
1	7.74	4.83	16.7	−4.1	4.1	−2.4	6.0
trans-**4**-OOH	8.17	5.05	16.4	−4.3	4.7	−3.6	8.5
trans-**5**-OOH	8.56	5.31	16.0	−1.0	6.8	−1.0	0.0

[a] Number of equivalent nuclei is given in parentheses. [b] **1**, *trans*-DEPMPO-OOH; **2**, *cis*-DEPMPO-OOH; **4** and **5**, deuterated DEPMPO derivatives, see structure in Scheme 1. [c] Nonresolved. [d] See eqs 1 and 2.

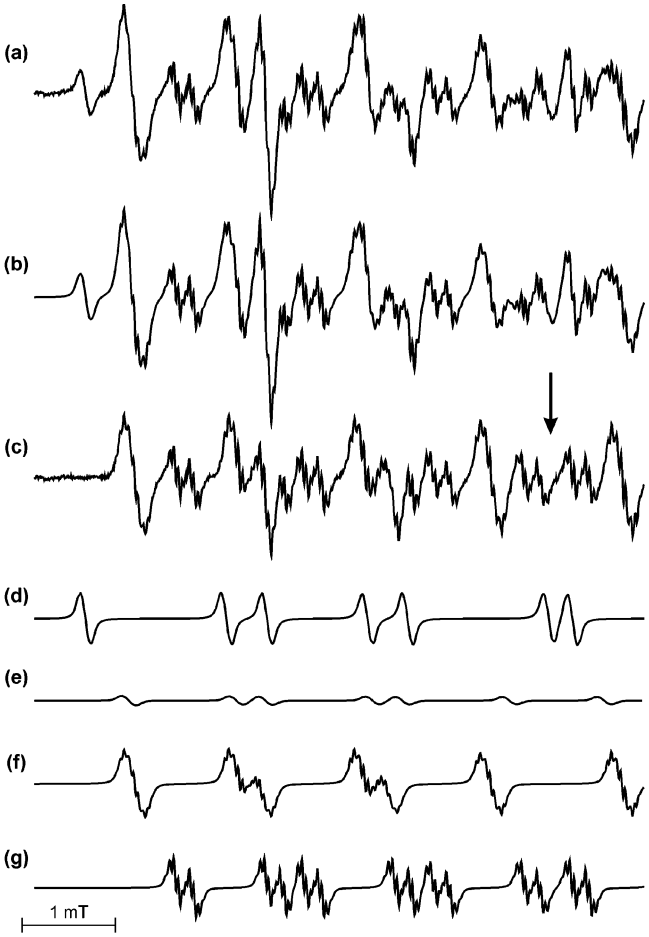

Figure 2. (a) Low-field half ESR spectrum obtained by mixing 30% H_2O_2 with 0.1 M DEPMPO in pyridine at 366 K; (b) simulation of (a); (c) after mathematical subtraction from (a) of reconstructed experimental signals of DEPMPO-R (R = alkyl) and DEPMPO-OH. (d−g) Calculated signal components of (b) at their actual relative concentrations: (d) DEPMPO-R; (e) DEPMPO-OH; (f) *trans*-DEPMPO-OOH; (g) *cis*-DEPMPO-OOH. The arrow indicates the position of the center of the spectra.

occur. A recognized unimolecular decomposition pathway for DEPMPO-OOH involves release of nitric oxide.[20] We have recently shown that its interaction with the nitrone yields the HO•/adduct (DEPMPO-OH) by a mechanism not involving a step where HO• is actually trapped.[21] This can explain why DEPMPO-OH is often detected as a byproduct during DEPMPO-OOH formation.[14,21]

(b) Different Forms of LWA. We have previously modeled the LWA in DEPMPO-OOH using the extended Bloch equations[22] and the relaxation dependence of the line width W[23]

$$W(M_N, M_P) = \alpha + \beta M_N + \gamma M_N^2 + \beta' M_P + \gamma' M_N M_P \quad (1)$$

where M_N and M_P are the magnetic quantum numbers of nitrogen and phosphorus nuclei, respectively, and $\alpha-\gamma'$ are the relaxation coefficients (see Table 1). Under conditions in which LWA is caused by a fast interconversion (i.e., $\tau^{-1} \gg \delta\omega$) between two sites (e.g., conformers), the line broadening δW is expressed by

$$\delta W = p_1 p_2 \delta\omega^2 t \quad (2)$$

where $\delta\omega$ is the frequency difference of the resonances for the two sites, τ is the exchange time, and p_1 and p_2 are the respective

SCHEME 2: Exchange Shifts in the Two-Site Model for Two $I = 1/2$ Spins

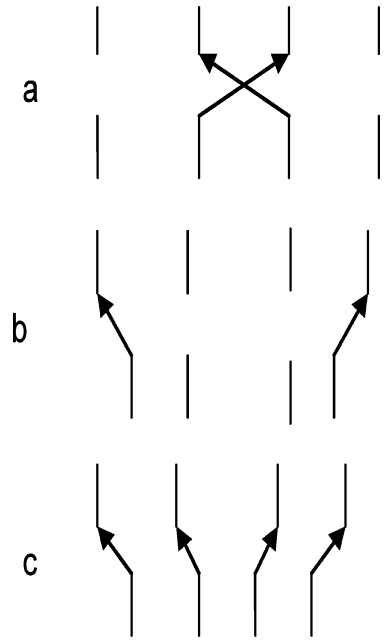

(a) Symmetry-related spins: normal LWA is caused by the constant sum of the couplings. (b) Nonequivalent spins: inverted LWA is caused by the constant difference of the couplings. (c) Nonequivalent spins: uniform broadening occurs when only one coupling is changing.

populations for T1 and T2.[22] When chemical exchange occurs in radicals bearing two mirror symmetric protons[22] or ^{31}P nuclei,[23] only the two inner lines of the ESR quartet structure show alterations of their line widths, whereas the outer lines remain unaffected because the molecular interconversion takes place between two symmetry-related sites giving a constant sum of the two coupling constants. This type of LWA can be termed as an exchange with constant sum of the couplings (Scheme 2a). The situation is opposite for any reported DEPMPOs-OOH adducts,[6,10,12−14,17] in which the low- and high-field lines are broad and the inner lines in the quartets (i.e., the ^{31}P doublet split by the H doublet) of the nitrogen triplets show superhyperfine splittings (see Figure 1). This type of LWA can be termed as an inverted LWA caused by the parallel change of coupling constants, i.e., for one of the sites A_P and A_H couplings are large, whereas for the other site both couplings are small and the differences of the couplings for the two nuclei are close (Scheme 2b). Consequently, the exchange shift caused by the molecular interconversion is large for the outer $M_P = M_H$ transitions and small for the inner $M_P = -M_H$ lines and therefore this inverted LWA can be termed as the exchange with constant difference of the couplings. Furthermore, significant LWA can be expected only if at least two nuclei have rather different couplings in the exchanging sites. The conformational interchange also occurs for DMPO-OOH, but as in this case, only the β-H coupling is changing significantly, no LWA but only a uniform broadening for all the lines occurs (Scheme 2c), which cannot be distinguished from the usual relaxation mechanism.[5] This broadening is indeed present, as evidenced by the lack of well-resolved superhyperfine structure in the spectrum of DMPO-OOH.

(c) LWA Analysis of DEPMPO-OOH Spectrum: Unexpected Ambiguities in the Fast Exchange Model. In the fast exchange limit, computer simulation of the LWA in DEPMPO-OOH yielded similar fits for other sets of hfcs than those reported in Table 1. If only the β-H and ^{31}P couplings differ in

the T1 and T2 sites while the g factor, A_N, and the γ-hfcs are considered constant and if differences in the relaxation contributions for the hyperfine lines are neglected, then the line positions of the (β-H/^{31}P) quartet are determined by the average couplings $<A> = p_1A_1 + p_2A_2$, whereas terms in the form of $p_1p_2(A_1 - A_2)^2\tau$ appear in the exchange broadening contribution, where $A_1 - A_2$ is proportional to the $\delta\omega$ used in eq 2. Because both above expressions are symmetric under interchanging p_1 and p_2, two solutions are obtained that can equally describe the line positions and the exchange broadenings for all lines. The two solutions should infer that both <A> and the difference $\Delta A = A_1 - A_2$ should be the same

$$<A> = p_1A'_1 + p_2A'_2 = p_2A''_1 + p_1A''_2 \quad (3a)$$

$$\Delta A = A'_1 - A'_2 = A''_1 - A''_2 \quad (3b)$$

where the indices $'$ and $''$indicate the two possible solutions. Equations 3a and 3b are fulfilled if

$$A''_1 = A'_1 + (p_1 - p_2)\Delta A \quad (4a)$$

$$A''_2 = A'_2 + (p_1 - p_2)\Delta A \quad (4b)$$

Equation 4 show that, in the fast exchange limit, it is not possible to determine which of the sites having either large A_P and A_H or small A_P and A_H has the largest population. In the following, these two possibilities will be termed L and S, respectively.

There is a further ambiguity, however, because of the quadratic nature of line broadening expression. In DEPMPOs-OOH, the width of the broad and narrow lines can be given as

$$W_{broad} = p_1p_2\tau(\Delta A_P + \Delta A_H)^2 \quad (5a)$$

$$W_{narrow} = p_1p_2\tau(\Delta A_P - \Delta A_H)^2 \quad (5b)$$

respectively. If we define ΔA_P and ΔA_H as positive quantities, then

$$\Delta A_P + \Delta A_H = \sqrt{\frac{W_{broad}}{p_1p_2\tau}} \quad (6a)$$

but $\Delta A_P - \Delta A_H$ could be either positive or negative

$$\Delta A_P - \Delta A_H = \pm\sqrt{\frac{W_{narrow}}{p_1p_2\tau}} \quad (6b)$$

Consequently, two couples of independent solutions exist, e.g.

$$\Delta A_P = \frac{\sqrt{W_{broad}} + \sqrt{W_{narrow}}}{2\sqrt{p_1p_2\tau}} \quad (7a)$$

$$\Delta A_P = \frac{\sqrt{W_{broad}} - \sqrt{W_{narrow}}}{2\sqrt{p_1p_2\tau}} \quad (7b)$$

or the expressions of eq 7 where ΔA_P and ΔA_H are interchanged. This second ambiguity expresses the fact that there is no way to determine which difference of the couplings ΔA_P or ΔA_H is the largest, leading to two possibilities termed P or H, respectively. Taken together, there are thus four equivalent solutions describing the LWA in DEPMPOs-OOH, i.e., LP, LH, SP, and SH. By using eq 4 and 7 we determined the other three sets of A_P and A_H values if one of the solutions has already been obtained by iteration of the adjustable parameters. These solutions could be only a first approximation, because A_N and the g factor could also be different in the two sites despite the fact that they are much less sensitive to the change in geometry and the relaxation affects the lines in the hyperfine patterns differently. In the case of the signal of **1** (Figure 1a), we thus carried out a full parameter optimization for the other three cases that yielded sets of hfcs and exchange parameters (Table 2), providing as good fits as for the first simulation (with the same correlation coefficients $r^2 \pm 0.001$, see Table 2).

TABLE 2: Calculated hfcs (in mT), Populations, and Exchange Parameters Deriving from Eqs 4 and 7 for the Two Conformers[a] of 1 at 296 K in Aqueous Buffer

param	LP[b]	LH	SP	SH
A_{P1}	5.306	5.208	4.764	4.834
A_{P2}	4.503	4.770	5.407	5.234
A_{H1}	1.262	1.516	0.961	0.827
A_{H2}	0.828	0.633	1.343	1.474
p_1	0.616	0.527	0.617	0.576
p_2	0.384	0.473	0.383	0.424
τ_1 (ns)	7.74	5.24	11.6	8.96
τ_2 (ns)	4.83	4.70	7.20	6.58
r_2	0.9957	0.9956	0.9945	0.9956

[a] Index "1" refers to the major conformer. [b] See text for the definitions.

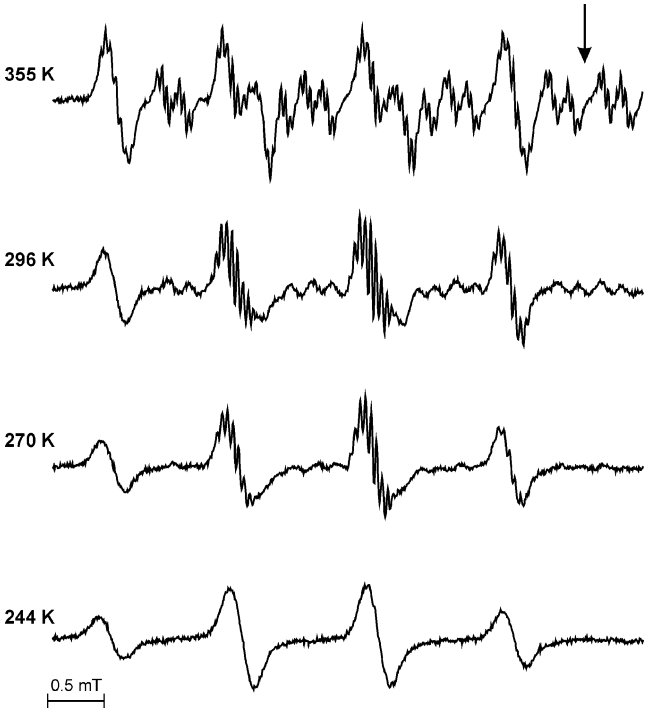

Figure 3. Temperature dependence of the DEPMPO-OOH signal in pyridine. The DEPMPO-R and DEPMPO-OH components were mathematically subtracted from the total signal. The arrow indicates the position of the center of the spectra.

(d) Analysis of the DEPMPO-OOH Spectra in Pyridine: A Thermodynamic Study of the Exchange Process by Using Two-Dimensional Simulation. Because the above four equivalent solutions only exist under fast exchange conditions, it is expected that only one of them will dominate in the case of slow exchange. At low temperatures, where this situation could be achieved, relaxation-induced line broadening will prevent the detection of individual lines for both sites. However, reaching a lower-temperature domain in which the exchange rate will be significantly decreased would help in discriminating the best solution. To extract the characteristic thermodynamic parameters of the exchange phenomenon, one has to use a solvent that allows us to record the ESR spectra of DEPMPO-OOH in a wide temperature range. This cannot be achieved in aqueous solution using an enzymatic $O_2^{\bullet-}$ generator (see Figure 3 in ref 6), and therefore, we generated DEPMPO-OOH by nucleophilic addition of H_2O_2 in pyridine,[24] for which the viscosity is low and the difference between freezing and boiling

points is large enough. Figure 2a shows the low-field part of the spectrum recorded at 366 K in pyridine which was simulated (Figure 2b) assuming four components, i.e., the expected **1** (49.0%) and **2** (21.2%), and the two additional adducts DEPMPO-OH ($A_N = 1.347$ mT; $A_P = 4.688$ mT; $A_{H\beta} = 1.058$ mT; $g = 2.00570$; 20.4%) and an alkyl adduct DEPMPO-R ($A_N = 1.386$ mT; $A_P = 4.787$ mT; $A_{H\beta} = 1.782$ mT; $g = 2.00540$; 9.4%). Unambiguous assignment of DEPMPO-OH has been performed by recording an authentic spectrum from a 1 mM Fe^{2+}-driven Fenton reaction on 0.1 M DEPMPO in 98.5% pyridine using 1 mM H_2O_2, the hfcs of which at 296 K ($A_N = 1.331$ mT; $A_P = 4.770$ mT; $A_{H\beta} = 1.015$ mT) closely matched that calculated in the nucleophilic addition experiments at the same temperature (data not shown). Figure 2d-g display the individual components of Figure 2b, revealing for the first time the superhyperfine structure of **2** except for the easily visible γ-doublet caused by the large splitting of one of the hydrogen atoms of C-3 (Figure 2 g). The simplicity of the DEPMPO-R and DEPMPO-OH spectral patterns (plots d and e in Figure 2, respectively) allowed us to use a reliable mathematical procedure to obtain the pure experimental signal of **1** + **2** (Figure 2c), which was introduced in the subsequent two-dimensional simulation procedure. In this model, the line shape is described by the solution of extended Bloch equations[22] and the temperature dependence of the exchange parameters is determined from the thermodynamic equations.[18] This requires a smaller number of adjustable parameters compared to the classical procedure in which all individual site populations and the exchange times should be determined from the ESR spectra at each temperature, and the thermodynamic or kinetic data are obtained by the respective Arrhenius fit. We recorded a series of intense and resolved spectra in the range 244−366 K, typical examples of which are shown in Figure 3 where the secondary signals were computer-eliminated as described above. In the two-dimensional analysis of these set of signals, we took into account that each ESR parameter will have an intrinsic temperature dependence, the variation being generally small for the *g* factors and long-range hfcs, intermediate for the large *N*, ^{31}P, and β-H hfcs, and rather large for the relaxation parameters. We assume, however, that for all parameters, the temperature dependence is smooth enough to be described by a power expansion containing no more than four *Q* terms

$$Q = \sum_{n=0}^{n\leq 3} Q_n (T - T_0)^n \tag{8}$$

In the computation, we chose $T_0 = 273$ K and adjusted parameters were $n = 2$ for the *g* factors and the small hfcs (i.e., γ-splittings), and $n = 3$ or 4 for the relaxation parameters and the other hfcs. The τ values (derived from the Arrhenius or Eyring eqs 9 and 10, respectively) and relative populations (calculated from the Van t'Hoff eq 11) were not adjusted for the individual spectra; instead the thermodynamic and kinetic parameters were adjusted to obtain the best overall fit for the whole spectrum series.

$$K = \frac{1}{\tau} = Ae - \frac{E_a}{RT} \tag{9}$$

$$K = \frac{k_B T}{h} e^{\frac{\Delta S^{\#}}{R}} e^{-\frac{\Delta H^{\#}}{RT}} \tag{10}$$

$$K = \frac{p_1}{p_2} = e^{\frac{\Delta S_R}{R} - \frac{\Delta H_R}{RT}} \tag{11}$$

In the two-dimensional curve fitting procedure, 118 nonlinear parameters were iterated (10 thermodynamic and 108 ESR coefficients). In spite of the large number of nonlinear parameters, the least-square fit presented a good stability due to the great amount of information provided by 15 spectra acquired above 273 K and containing more than 100 well-resolved lines. We used a combination of iteration procedures described earlier to determine the minimum of the least-square deviation between experimental and calculated spectra set.[17] The critical part of nonlinear parameter adjustment was the preliminary choice of an appropriate starting parameter set among the four possible solutions yielded by one-dimensional calculations in the case of fast exchange (Table 2). These solutions were discriminated by the initial choice of Q_0 and Q_1 for the crucial couplings A_P and A_H, whereas $Q_2 = Q_3 = 0$ was assumed (see eq 8). The best overall fits were obtained using the LP model. Whereas strong LWA was still observed for **1** at 366 K (Figure 2f), the spectrum of **2** was always symmetric (see Figure 2 g). At high temperatures, the recording of intense and resolved spectra for **2** therefore allowed us to show that it is also subjected to a conformational exchange, yielding a uniform broadening of the ESR lines as depicted in Scheme 2c, a phenomenon that could not be observed at room temperature (see Figure 1a and Table 1). The ρ = **2**:**1** concentration ratio presented a large and reversible change with temperature: although it was nearly zero below 273 K, it reached 0.17 at room temperature and an exceptionally large value of 0.4 at 366 K. Cooling down to room temperature a sample having $\rho = 0.4$ restored the same diastereoisomer ratio that was observed before heating of the sample (e.g., $\rho = 0.19$, data not shown) suggesting that the rate of nucleophilic addition plays a dominant role rather than the difference in decay rates.

TABLE 3: Thermodynamic Parameters of the Equilibrium between T1 and T2 Conformers of DEPMPO-OOH Diastereoisomers in Pyridine[a]

	1	**2**
ΔH_R (kJ/mol)	−0.68	−2.49
ΔS_R (J/mol.K)	3.79	−3.35
ΔG_R (kJ/mol)	−1.81	−1.49
E_a (kJ/mol)	21.11	24.96
$\Delta H^{\#}$ (kJ/mol)	18.52	24.05
$\Delta S^{\#}$ (J/mol.K)	−14.86	−0.66
$\Delta G^{\#}$ (kJ/mol)	22.95	24.25

[a] ΔH, ΔS, and ΔG (given at 298 K) were derived from the Eyring or Van t'Hoff equations, and E_a was calculated from the Arrhenius equation.

Table 3 shows the thermodynamical data afforded by two-dimensional analysis. The two interconversion barriers between T1 and T2 are in agreement with that calculated by density functional theory studies for the rotation around the O−O bond in various molecules, including H_2O_2.[25] On the basis of spectroscopic studies, a well-accepted model[25b−d,26] to explain the high potential barrier hindering the torsional oscillation around the O−O bond in peroxides (e.g., about 17 kJ/mol in H_2O_2[25a]) involves a combination of the electrostatic repulsion between the oxygen lone pairs, their hyperconjugation with the adjacent antibonding σ^* bonds, and steric effects, all interactions globally favoring two gauche conformers rather than a planar geometry. We can reasonably argue that the phenomenon causing LWA in the spectrum of **1** has at least this rotational component.[17,23] Although it looks plausible that the rotation around the O−O bond may be solely responsible for the LWA seen in the DEPMPOs-OOH and DEPMPOs-OOR spectra (e.g., it was also reported for the MeOO• and tBuOO• adducts[12b,d,e,g]), other rotational motions could contribute at a lower extent. The two pseudo-rotational conformers in β-substituted pyrrolidinyloxyls have geometries close to $^3T_4$ and $^4T_3$ in the [E_3−^4E] and [^3E−E_4] domains, with a low interconversion barrier of about 10 kJ/mol precluding any observation of a chemical exchange by ESR.[27] The involvement of hindered rotation around the

TABLE 4: Calculated hfcs (in mT),[a] Relaxation Parameters (in μT), Populations, and Exchange Times (in ns) of DEPMPO-OOH Diastereoisomers at 296 K in Pyridine

	1		**2**	
	conformers			
	T1	T2	T1	T2
A_N	1.206	1.250	1.257	1.270
A_P	5.200	4.488	3.557	4.269
$A_{H\beta}$	1.266	0.605	0.907	0.883
A_{Me}	0.045	0.045	0.040	0.040
$A_{H\gamma}$(3-C)[b]	0.096	0.096	0.157	0.157
$A_{H\gamma}$(3-C)	0.056	0.056	0.005 [c]	0.005 [c]
$A_{H\gamma}$(4-C)	0.046	0.046	0.045	0.045
$A_{H\gamma}$(4-C)	0.035	0.035	0.028	0.028
α	24.7	24.7	19.0	19.0
β	−3.6	−3.6	−3.1	−3.1
γ'	3.1	3.1	2.6	2.6
β'	−1.9	−1.9	0.4	0.4
γ'	4.7	4.7	0.9	0.9
p (%)	67.4	32.6	64.8	35.2
τ	2.40	1.16	4.41	2.40
g	2.00707	2.00693	2.00715	2.00695

[a] Error estimates for **1** (**2**) are as follows: hfcs, 0.1 (0.2) mT; g values, 5×10^{-5} (10^{-4}). [b] γ-Couplings and relaxation parameters were taken to be identical for the two conformers. [c] Estimated.

C-2−O bond as a cause of exchange in DEPMPOs-OOR can also be excluded, because neither the hydroxyl nor alkoxyl adducts of DEPMPOs present temperature-dependent LWA even under conditions allowing the recording of superhyperfine structure (e.g., in DEPMPO-OH[14] and DEPMPO-OMe[16]). Indeed, density functional theory calculations predicted a barrier close to 40 kJ/mol for the rotation around the C-2−O bond in DMPO-OOH,[28] rendering this kind of motion slow in the ESR time scale.

Table 4 reports the ESR parameters for **1** and **2** at 296 K optimized by the two-dimensional analysis. The trans configuration in **1**, which allows the phosphoryl and OOH groups to occupy preferential pseudoaxial orientations, stabilizes the adduct by anomeric interactions.[12e] Because β-couplings in pyrrolidinyloxyls follow dihedral rules,[29] the large A_P and low β-hydrogen couplings in the T1 conformer of **1** show a distortion of the ground $^3T_4$ twist geometry of the pyrrolidine ring toward an intermediate $<^3E-E_4>$ situation, while lower values for these constants in the T2 conformer reveal a ^3E-like distorted geometry (Scheme 3). The similar and low β-hydrogen couplings and the rather low A_P values in the two conformers of **2** indicate that it is the OOH group that retains an axial position, minimizing steric interactions. Thus in the case of **2**, $<^3E-E_4>$ and ^3E-like distorted geometries seem reasonable for T1 and T2, respectively (Scheme 3).

There is increasing interest in intramolecular stabilizing effects in DEPMPO adducts such as DEPMPO-OOH[15] and DEPMPO-OH. We recently brought experimental evidence of an increased stability of *cis*- versus *trans*-DEPMPO-OH, which was predicted[30] to rely on significant internal H bonding between the hydroxyl and the phosphoryl groups in the *cis* diastereoisomer. Interestingly, density functional theory calculations[5,28] postulated two major O−O rotamers for DMPO-OOH characterized by the different orientation of the hydroperoxyl hydrogen, directed either toward or opposite relative to the nitroxyl function. Because an intramolecular H bond has been proposed[7,28] to explain the enhanced stability of the former DMPO-OOH rotamer, we speculate by analogy that a similar stabilization occurs between the T1 and T2 O−O rotamers of **1** and **2**, as depicted in Scheme 3.

4. Conclusions

Specific deuteration of DEPMPO allowed the complete characterization in aqueous solution of long-range couplings in DEPMPO-OOH. The two-dimensional analysis of the temperature-dependent spectra led to the determination of the thermodynamic and kinetic parameters of the conformational exchange showing (i) that the simultaneous variations of A_P and A_H couplings generate a marked LWA in *trans*-DEPMPO-OOH, and (ii) that in *cis*-DEPMPO-OOH, uniform line broadening occurs as the result of the only significant change in A_P coupling. Both phenomena result from changes in the five-membered-ring geometry caused by the different character of the interaction

SCHEME 3: Representative Potential Curves and Geometries for the Exchanging Conformers of DEPMPO-OOH Diastereoisomers

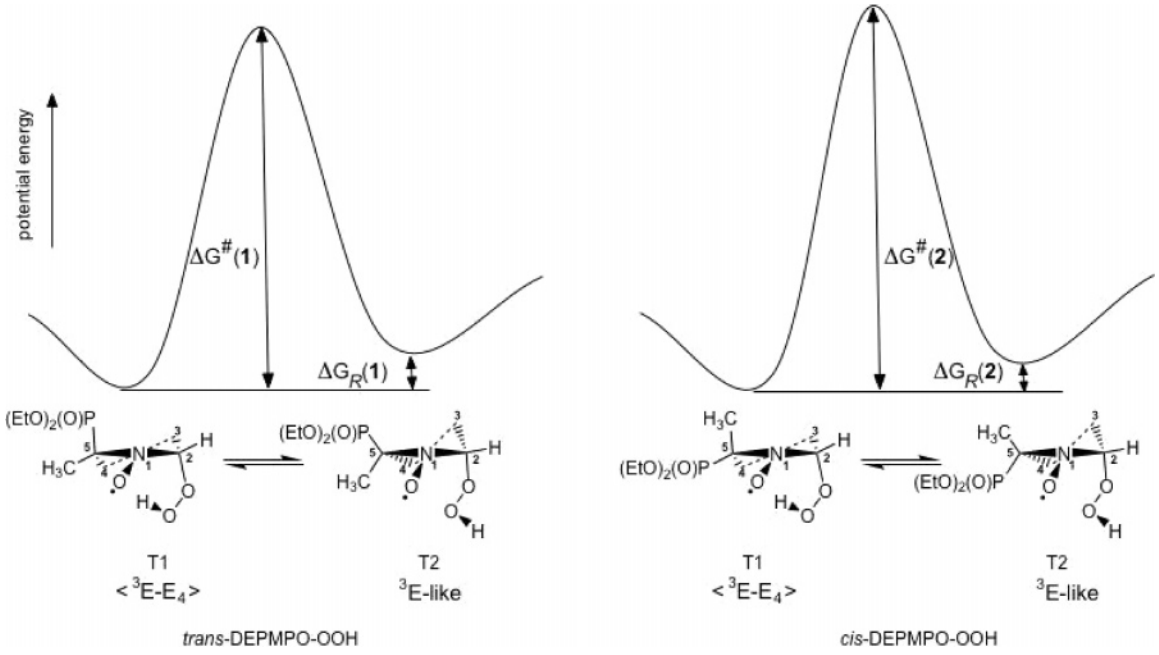

between the ring and the OH group having two preferential orientations in the course of rotation around the O−O bond.

Acknowledgment. A.R. expresses his thanks for the partial financial support of the Hungarian Scientific Research Fund OTKA (Grant T-046953) and the Grant NKFP 1/A/005/2004 "MediChem2".

References and Notes

(1) (a) *Spin Labeling: Theory and Applications*; Berliner, L. J., Ed.; Academic Press: New York, 1976. (b) *Spin Labeling: Theory and Applications II*; Berliner, L. J., Ed.; Academic Press: New York, 1979. (c) Hubbel, W. L.; Cafiso, D. S.; Altenbach, C. *Nat. Struct. Biol.* **2000**, *7*, 735.

(2) Harbour, J. R.; Chow, V.; Bolton, J. R. *Can. J. Chem.* **1974**, *52*, 3549.

(3) Buettner, G. R. *Free Radical Res. Commun.* **1990**, *10*, 11.

(4) Rosen, G. M.; Beselman, A.; Tsai, P.; Pou, S.; Mailer, C.; Ichikawa, K.; Robinson, B. H.; Nielsen, R.; Halpern, H. J.; MacKerell, A. D. *J. Org. Chem.* **2004**, *69*, 1321.

(5) Clément, J. L.; Ferré, N.; Siri, D.; Karoui, H.; Rockenbauer, A.; Tordo, P. *J. Org. Chem.* **2005**, *70*, 1198.

(6) Dikalov, S.; Jiang, J.; Mason, R. P. *Free Radical Res.* **2005**, *39*, 825.

(7) Villamena, F. A.; Merle, J. K.; Hadad, C. M.; Zweier, J. L. *J. Phys. Chem. A.* **2005**, *109*, 6089.

(8) (a) Buettner, G. R.; Oberley, L. W. *Biochem. Biophys. Res. Commun.* **1978**, *83*, 69. (b) Finkelstein, E.; Rosen, G. M.; Rauckman, E. J.; Paxton, J. *Mol. Pharmacol.* **1979**, *16*, 676.

(9) Sturgeon, B. E.; Chen, Y. R.; Mason, R. P. *Anal. Chem.* **2003**, *75*, 5006.

(10) Fréjaville, C.; Karoui, H.; Tuccio, B.; Le Moigne, F.; Culcasi, M.; Pietri, S.; Lauricella, R.; Tordo, P. *J. Med. Chem.* **1995**, *38*, 258.

(11) Pou, S.; Rosen, G. M.; Wu, Y.; Keana, F. W. *J. Org. Chem.* **1990**, *55*, 4438.

(12) (a) Olive, G.; Le Moigne, F.; Mercier, A.; Rockenbauer, A.; Tordo, P. *J. Org. Chem.* **1998**, *63*, 9095. (b) Karoui, H.; Nsanzumuhire, C.; Le Moigne, F.; Tordo, P. *J. Org. Chem.* **1999**, *64*, 1471. (c) Clément, J. L.; Barbati, S.; Fréjaville, C.; Rockenbauer, A.; Tordo, P. *J. Chem. Soc., Perkin Trans. 2* **2001**, 1471. (d) Chalier, F.; Tordo, P. *J. Chem. Soc., Perkin Trans. 2* **2002**, 2110. (e) Nsanzumuhire, C.; Clément, J. L.; Ouari, O.; Karoui, H.; Finet, J. P.; Tordo, P. *Tetrahedron Lett.* **2004**, 6385. (f) Hardy, M.; Chalier, F.; Finet, J. P.; Rockenbauer, A.; Tordo, P. *J. Org. Chem.* **2005**, *70*, 2135. (g) Hardy, M.; Ouari, O.; Charles, L.; Finet, J. P.; Iacazio, G.; Monnier, V.; Rockenbauer, A.; Tordo, P. *J. Org. Chem.* **2005**, *70*, 10426. (h) Hardy, M.; Chalier, F.; Ouari, O.; Finet, J. P.; Rockenbauer, A.; Kalyanaraman, B.; Tordo, P. *Chem. Commun.* **2007**, 1083.

(13) (a) Stolze, K.; Udilova, N.; Nohl, H. *Free Radical Biol. Med.* **2000**, *29*, 1005. (b) Xu, Y. K.; Chen, Z. W.; Sun, J.; Liu, K.; Chen, W.; Shi, W.; Wang, H. M.; Liu, Y. *J. Org. Chem.* **2002**, *67*, 7624. (c) Shioji, K.; Tsukimoto, S.; Tanaka, H.; Okuma, K. *Chem. Lett.* **2003**, *32*, 604.

(14) Culcasi, M.; Rockenbauer, A.; Mercier, A.; Clément, J. L.; Pietri, S. *Free Radical Biol. Med.* **2006**, *40*, 1524.

(15) (a) Villamena, F. A.; Rockenbauer, A.; Gallucci, J.; Velayutham, M.; Hadad, C. M.; Zweier, J. L. *J. Org. Chem.* **2004**, *69*, 7994; supporting information S37−S40. (b) Villamena, F. A.; Hadad, C. M.; Zweier, J. L. *J. Phys. Chem. A* **2005**, *109*, 1662.

(16) Dikalov, S.; Tordo, P.; Motten, A.; Mason, R. P. *Free Radical Res.* **2003**, *37*, 705.

(17) (a) Rockenbauer, A.; Korecz, L. *Appl. Magn. Reson.* **1996**, *10*, 29. (b) Rockenbauer, A. *Mol. Phys. Rep.* **1999**, *26*, 117.

(18) Rockenbauer, A.; Nagy, N. V.; Le Moigne, F.; Gigmes, D.; Tordo, P. *J. Phys. Chem. A* **2006**, *110*, 9542.

(19) Clément, J. L.; Finet, J. P.; Fréjaville, C.; Tordo, P. *Org. Biomol. Chem.* **2003**, *1*, 1591.

(20) Locigno, E. J.; Zweier, J. L.; Villamena, F. A. *Org. Biomol. Chem.* **2005**, *3*, 3220.

(21) Culcasi, M.; Muller, A.; Mercier, A.; Clément, J. L.; Payet, O.; Rockenbauer, A.; Marchand, V.; Pietri, S. *Chem. Biol. Interact.* **2006**, *164*, 215.

(22) Atherton, N. M. *Electron Spin Resonance, Theory and Application*; Wiley & Sons: New York, 1973.

(23) Rockenbauer, A.; Gaudel-Siri, A.; Siri, D.; Berchadsky, Y.; Le, Moigne, F.; Olive, G.; Tordo, P. *J. Phys. Chem. A* **2003**, *107*, 3851.

(24) (a) Reszka, K.; Chignell, C. F. *Free Radical Res. Commun.* **1991**, *14*, 97. (b) Reszka, C.; Bilski, P.; Chignell, C. F. *Free Radical Res. Commun.* **1992**, *17*, 377.

(25) (a) Giguere, P. A. *J. Chem. Phys.* **1950**, *18*, 88. (b) Hunt, R. H.; Leacock, R. A.; Peters, C. W.; Hecht, K. T. *J. Chem. Phys.* **1965**, *42*, 1931. (c) Khursan, S. L.; Antonovsky, V. L. *Russ. Chem. Bull.* **2003**, *52*, 1908. (d) Khursan, S. L.; Antonovsky, V. L. *Russ. Chem. Bull.* **2003**, *52*, 1312.

(26) (a) Sebbar, N.; Bockhorn, H.; Bozzelli, J. W. *Phys. Chem. Chem. Phys.* **2002**, *4*, 3691. (b) Sebbar, N.; Bozzelli, J. W.; Bockhorn, H. *J. Phys. Chem. A* **2004**, *108*, 8353. (c) Sun, H.; Bozzelli, J. W. *J. Phys. Chem. A* **2003**, *107*, 1018.

(27) Rockenbauer, A.; Korecz, L.; Hideg, K. *J. Chem. Soc., Perkin Trans. 2* **1993**, 2149.

(28) Villamena, F. A.; Merle, J. K.; Hadad, C. M.; Zweier, J. L. *J. Phys. Chem. A* **2005**, *109*, 6083.

(29) Rockenbauer, A.; Györ, M.; Hankovsky, H. O.; Hideg, K. ESR study of the conformation of 5- and 6-membered cyclic nitroxides (aminoxyl) radicals. In *Electron Spin Resonance*; Symons, M. C. R., Ed.; Royal Society of Chemistry: Cambridge, UK, 1988; Vol. 11A, p 145.

(30) (a) Villamena, F. A.; Hadad, C. M.; Zweier, J. L. *J. Phys. Chem. A* **2003**, *107*, 4407. (b) Villamena, F. A.; Hadad, C. M.; Zweier, J. L. *J. Am. Chem. Soc.* **2004**, *126*, 1816.